

Effective field theory for the Ising model with a fluctuating exchange integral in an asymmetric bimodal random magnetic field: A differential operator technique

Ioannis A. Hadjiagapiou *

Section of Solid State Physics, Department of Physics, University of Athens, Panepistimiopolis, GR 15784 Zografos, Athens, Greece

Abstract

The spin-1/2 Ising model on a square lattice, with fluctuating bond interactions between nearest neighbors and in the presence of a random magnetic field, is investigated within the framework of the effective field theory based on the use of the differential operator relation. The random field is drawn from the asymmetric and anisotropic bimodal probability distribution $P(h_i) = p\delta(h_i - h_1) + q\delta(h_i + ch_1)$, where the site probabilities p, q take on values within the interval $[0, 1]$ with the constraint $p + q = 1$; h_i is the random field variable with strength h_1 and c the competition parameter, which is the ratio of the strength of the random magnetic field in the two principal directions $+z$ and $-z$; c is considered to be positive resulting in competing random fields. The fluctuating bond is drawn from the symmetric but anisotropic bimodal probability distribution $P(J_{ij}) = \frac{1}{2}\{\delta(J_{ij} - (J + \Delta)) + \delta(J_{ij} - (J - \Delta))\}$, where J and Δ represent the average value and standard deviation of J_{ij} , respectively. We estimate the transition temperatures, phase diagrams (for various values of system's parameters c, p, h_1, Δ), susceptibility, equilibrium equation for magnetization, which is solved in order to determine the magnetization profile with respect to T and h_1 .

Key words: Ising model, fluctuating pair interactions, asymmetric bimodal random field, effective field theory, phase diagram, phase transitions, magnetization

PACS: 05.50.+q, 75.10.Hk, 75.10.Nr, 75.50.Lk

* Corresponding author.

Email address: ihatziag@phys.uoa.gr (Ioannis A. Hadjiagapiou).

1 Introduction

Prediction of the critical behavior of modified spin models in the presence of site or bond dilution, random bonds, random fields has been the subject of many studies in the last decades; this modification brings about considerable changes in the critical behavior of these systems, such as replacement of a first-order phase transition (FOPT) by a second-order phase transition (SOPT), depression of tricritical points and critical end points, new critical points and universality classes, etc [1,2,3]. The study of the aforementioned disordered systems is based on the standard models, such as Ising, Blume-Capel, Baxter-Wu, Heisenberg, etc, modified accordingly to meet the requirements under consideration. Furthermore, extensions and versions of these models can be applied to describe many other different situations, such as multicomponent fluids, ternary alloys, ^3He - ^4He mixtures, in addition to the magnetic systems for which these were initially conceived. The most extensively investigated model in statistical and condensed matter physics is the spin-1/2 Ising model (IM), since its two dimensional version, without an external magnetic field, was analytically solved by Onsager; it is a simple one relative to other models of cooperative phenomena and has a wide range of applicability to real physical systems. Its three-dimensional version has not yet been solved exactly, for which the only existing results are either from the renormalization group calculations or series expansions and are thus considered to be the "exact" ones. In its modified versions, it exhibits a variety of multicritical phenomena, such as a phase diagram with ordered ferromagnetic and disordered paramagnetic phases separated by a transition line that changes from an SOPT to an FOPT joined at a tricritical point (TCP); besides these, critical points, critical end points, ordered critical points of various orders, re-entrance can appear as in the presence of random fields. The multicritical phenomena appear in systems presenting competition among distinct types of ordering and there are numerous circumstances in which this kind of phenomenon can arise. In ferromagnetic systems in the presence of random fields, the competition is between the parallel and random ordering, causing, occasionally, the conversion of a continuous transition into an FOPT and the subsequent appearance of TCP as well as re-entrance in some cases [4]. Random field effects on magnetic systems have been systematically studied not only for their own theoretical study but for their experimental importance, as well.

The methods used for the study of the IM are the mean field approximation (MFA), high temperature expansions, series expansion, renormalization group, Monte Carlo, effective field theory (EFT). The eldest one is the MFA, which is very popular because of its simplicity and has played an important role for the description of cooperative phenomena for many years; it gives qualitative agreement with experimental results for many of the physical quantities involved in a phase transition. However, MFA has some unsatisfactory results

in describing correctly the critical region because of the omission of correlations when its results are compared with those of experiments. MFA is still implemented because it is not complicated and can give a general view of the expected behavior for the system under consideration. Many efforts were attempted towards improving MFA, such as the effective field theory by Honmura and Kaneyoshi [5]. EFT relies on introducing a differential operator into the exact spin correlation function identities obtained by Callen [6] and using the van der Waerden spin identities, which improves substantially on the standard MFA [7,8]. The EFT approach is general and may be applied to systems with any spin value, adapting the van der Waerden identities accordingly. This procedure presents a great versatility and has been applied to several occasions such as pure, site- and bond-random Ising model, although this procedure shall not yield accurate values for the physical quantities in the critical region due to the absence of long range fluctuations. EFT has already been used in numerous physical problems as a tool to study the magnetic behavior of complex spin systems, such as diluted ferromagnets [9,10,11], pure anisotropic systems [12], disordered systems [13,14], cylindrical nanowires [15].

The Hamiltonian we shall adopt is that of Ising model with nearest neighbor interactions, in which the bond J_{ij} between two neighboring spins varies from pair to pair randomly; the system is also under the influence of a random field h_i , varying from site to site; both random variables are drawn from a suitable probability distribution function (PDF).

The Hamiltonian describing the above system is

$$H = - \sum_{\langle i,j \rangle} J_{ij} S_i S_j - \sum_i h_i S_i , \quad S_i = \pm 1 \quad (1)$$

The summation in the first term extends over all nearest neighbors and is denoted by $\langle i, j \rangle$; in the second term h_i represents a random field that couples to the one dimensional spin variable S_i . The Hamiltonian describes the competition between the long-range order (expressed by the first summation) and the random ordering fields. The presence of random fields requires two averaging procedures, the usual thermal average, denoted by angular brackets $\langle \dots \rangle$ and disorder average over the random fields denoted by $\langle \dots \rangle_r$ for the respective PDF's, which are usually a version of the bimodal or Gaussian distributions.

The random exchange integral J_{ij} between the sites i and j is drawn from the symmetric and anisotropic bimodal PDF,

$$P(J_{ij}) = \frac{1}{2} \{ \delta(J_{ij} - (J + \Delta)) + \delta(J_{ij} - (J - \Delta)) \} \quad (2)$$

where J and Δ represent the average value and standard deviation of J_{ij} , respectively, implying that the exchange integral is fluctuating. This choice of the PDF implies that both values ($J - \Delta, J + \Delta$) of the random exchange integral are equally probable.

The PDF for the random fields h_i is also of the bimodal type

$$P(h_i) = p\delta(h_i - h_1) + q\delta(h_i + h_2) \quad (3)$$

where $h_2 = ch_1$, c is the competition parameter and is considered to be positive so that the random fields are competitive. The site probability p is the fraction of lattice sites having a random magnetic field with strength h_1 , while the rest sites have a field with strength $(-h_2)$ with site probability q such that $p + q = 1$ and the usual choice was $p = q = \frac{1}{2}$, symmetric case, [4,16,17,18]. As far as the PDF (3) is non symmetric, the mean value for h_i does not vanish a priori, but, instead, is $\langle h_i \rangle_h = (p - cq)h_1$; an immediate result is that the system is under the influence of a magnetic field in case $p \neq q$ and $c \neq 1.0$.

One of the main issues was the experimental realization of random fields. Fishman and Aharony [19] showed that the randomly quenched exchange interactions Ising antiferromagnet in a uniform field H is equivalent to a ferromagnet in a random field with the strength of the random field linearly proportional to the induced magnetization. This identification gave new impetus to the study of the RFIM, the investigation gained further interest and was intensified resulting in a large number of publications (theoretical, numerical, Monte Carlo simulations and experimental) in the last thirty years. Although much effort had been invested towards this direction, the only well-established conclusion drawn was the existence of a phase transition for $d \geq 3$ (d space dimension), that is, the critical lower dimension d_l is 2 after a long controversial discussion [20], while many other issues are still unanswered; among them is the order of the phase transition (first or second order), the universality class and the dependence of these points on the form of the random field PDF. The study of RFIM has also highlighted another feature of the model, that of tricriticality and its dependence on the assumed distribution function of the random fields. According to the mean field approximation, the choice of the random field distribution can lead to a continuous FM/PM boundary as in the single Gaussian probability distribution, whereas for the bimodal one this boundary is divided into two parts, an SOPT branch for high temperatures and an FOPT branch for low temperatures separated by a TCP at $kT_c^t/(zJ) = 2/3$ and $h_c^t/(zJ) = (kT_c^t/(zJ)) \times \arg \tanh(1/\sqrt{3}) \simeq 0.439$ [16], where z is the coordination number and k the Boltzmann constant, such that for $T < T_c^t$ and $h > h_c^t$ the transition to the FM phase is first order for the symmetric case $p = \frac{1}{2}$. However, this behavior is not fully elucidated since in the case of the three-dimensional RFIM, the high temperature series expansions by Gofman et al [21] yielded only continuous transitions for both probability distribu-

tions, whereas according to Houghton et al [22] both distributions predicted the existence of a tricritical point, with $h_c^t = 0.28 \pm 0.01$ and $T_c^t = 0.49 \pm 0.03$ for the bimodal and $\sigma_c^t = 0.36 \pm 0.01$ and $T_c^t = 0.36 \pm 0.04$ for the single Gaussian. In the Monte Carlo studies for $d = 3$, Machta et al [23], using single Gaussian distribution, could not reach a definite conclusion concerning the nature of the transition, since for some realizations of randomness the magnetization histogram was two-peaked (implying an SOPT) whereas for other ones three-peaked, implying an FOPT.

In this investigation, we study the EFT applied to the random field spin-1/2 Ising model on a square lattice with random bond nearest neighbor interactions, calculating the relevant thermodynamic quantities, such as critical temperatures, susceptibility, magnetization profiles with respect to the temperature T and random field h_1 . The paper is organized as follows: In the next section, the EFT formalism is introduced and applied to the Ising model in the presence of a random field and random bonds interactions; the equation of state for the magnetization is derived. In section 3, the phase diagrams and magnetization profiles are calculated as functions of system's parameters; we close with the conclusions in section 4.

2 Model and formalism

Considering the Hamiltonian (1), each spin is under the influence of a molecular field \tilde{h}_i

$$\tilde{h}_i = \sum_{j=1}^z J_{ij} S_j + h_i \quad (4)$$

where z is the coordination number. For the current model the starting point is the Callen exact spin correlation function identity [6]

$$\langle\langle S_i \rangle\rangle_r = \langle\langle \tanh \left[\beta \sum_{j=1}^z J_{ij} S_j + \beta h_i \right] \rangle\rangle_r \quad (5)$$

where the summation takes all the nearest neighboring spin sites of i and $\langle\langle \dots \rangle\rangle_r$ indicates the thermal and random configurational averages. Following Honmura and Kaneyoshi [5], introducing the differential operator $D \equiv \frac{\partial}{\partial x}$ into (5) and using also the van der Waerden identity

$$e^{J_{ij} S_j D} = \cosh(J_{ij} D) + S_j \sinh(J_{ij} D) \quad (6)$$

Eq. (5) transforms into

$$\begin{aligned}
\langle\langle S_i \rangle\rangle_r &= \langle\langle \exp \left[\beta D \sum_{j=1}^z J_{ij} S_j \right] \rangle\rangle_r \langle \tanh [x + \beta h_i] \rangle_{x=0} \\
&= \langle\langle \prod_{j=1}^z [\cosh(\beta J_{ij} D) + S_j \sinh(\beta J_{ij} D)] \rangle\rangle_r f(x, \beta h_i)_{x=0}
\end{aligned} \tag{7}$$

where

$$f(x, \beta h_i) = p \tanh(x + \beta h_1) + q \tanh(x - \beta h_2) \tag{8}$$

Before proceeding to the calculations, we shall consider the following approximations to make the problem mathematically tractable, (a) the configurational average of spins and exchange integral are taken independently, $\langle\langle S_j f(J_{ij}) \rangle\rangle \simeq \langle\langle S_j \rangle\rangle \langle\langle f(J_{ij}) \rangle\rangle$, (b) the exchange integrals J_{ij} for different j 's are also independent of each other, $\langle\langle f_1(J_{ij}) f_2(J_{ik}) \rangle\rangle = \langle\langle f_1(J_{ij}) \rangle\rangle \langle\langle f_2(J_{ik}) \rangle\rangle$. Under these assumptions the relation (7) is written as

$$\langle\langle S_i \rangle\rangle_r \simeq \sum_{n=1}^z Q_{nz} \sum_{j_1, j_2, \dots, j_n=1}^z \langle\langle S_{j_1} S_{j_2} \dots S_{j_n} \rangle\rangle_r \tag{9}$$

where all the spins $S_{j_1}, S_{j_2}, \dots, S_{j_n}$ are nearest neighbors of S_i and the coefficient Q_{nz} is

$$Q_{nz} = \langle \cosh(\beta D J_{ij}) \rangle^{z-n} \langle \sinh(\beta D J_{ij}) \rangle^n f(x, \beta h_i)_{x=0} \tag{10}$$

As far as the $\tanh(x)$ is an odd function of its argument, only odd n appear in Q_{nz} for the square ($z = 4$) lattice. Considering the PDF (2) for J_{ij} , the averages in (10) are

$$\begin{aligned}
\langle \cosh(\beta D J_{ij}) \rangle &= \cosh(\beta J D) \cosh(\beta \Delta D) \\
\langle \sinh(\beta D J_{ij}) \rangle &= \sinh(\beta J D) \cosh(\beta \Delta D)
\end{aligned} \tag{11}$$

thus (10) becomes

$$Q_{nz} = \cosh^{z-n}(\beta J D) \sinh^n(\beta J D) \cosh^z(\beta \Delta D) f(x, \beta h_i)_{x=0} \tag{12}$$

which, for even z , takes the form

$$Q_{nz} = \sum_{\ell=1}^{z/2} b_{\ell}^{(n)} \sinh(2\ell \beta J D) \sum_{\nu=0}^{z/2} |a_{\nu}^{(z)}| \cosh(2\nu \beta \Delta D) f(x, \beta h_i)_{x=0}$$

$$= \sum_{\ell=1}^{z/2} b_{\ell}^{(n)} \sum_{\nu=0}^{z/2} |a_{\nu}^{(z)}| \sinh(2\ell\beta JD) \cosh(2\nu\beta\Delta D) f(x, \beta h_i)_{x=0} \quad (13)$$

using the operator relation $e^{wD} f(x) = f(x + w)$, we obtain for the summand in (13)

$$\begin{aligned} & \sinh(2\ell\beta JD) \cosh(2\nu\beta\Delta D) f(x, \beta h_i)_{x=0} = \\ & \frac{1}{4} \left\{ p \left(\tanh[\beta(2\ell J + 2\nu\Delta + h_1)] + \tanh[\beta(2\ell J - 2\nu\Delta + h_1)] + \right. \right. \\ & \quad \left. \tanh[\beta(2\ell J - 2\nu\Delta - h_1)] + \tanh[\beta(2\ell J + 2\nu\Delta - h_1)] \right) + \\ & \quad q \left(\tanh[\beta(2\ell J + 2\nu\Delta - h_2)] \tanh[\beta(2\ell J - 2\nu\Delta - h_2)] + \right. \\ & \quad \left. \tanh[\beta(2\ell J - 2\nu\Delta + h_2)] + \tanh[\beta(2\ell J + 2\nu\Delta + h_2)] \right) \left. \right\} \\ & \equiv \frac{1}{4} g_{\ell\nu}(\beta, J, \Delta, h_1, h_2) \quad (14) \end{aligned}$$

thus Eq. (13) is written as

$$Q_{nz} = \frac{1}{4} \sum_{\ell=1}^{z/2} b_{\ell}^{(n)} \sum_{\nu=0}^{z/2} |a_{\nu}^{(z)}| g_{\ell\nu}(\beta, J, \Delta, h_1, h_2) \quad (15)$$

with

$$\begin{aligned} a_{\nu}^{(z)} &= \frac{2 - \delta_{\nu,0}}{2^z} (-1)^{\frac{z}{2} - \nu} \binom{z}{\frac{z}{2} - \nu} \\ b_{\ell}^{(1)} &= \frac{2\ell}{z} |a_{\ell}^{(z)}| \\ b_{\ell}^{(3)} &= \frac{2\ell}{\prod_{i=0}^2 (z - i)} [(2\ell)^2 - (3z - 2)] |a_{\ell}^{(z)}| \\ b_{\ell}^{(5)} &= \frac{2\ell}{\prod_{i=0}^4 (z - i)} [(2\ell)^4 - 10(z - 2)(2\ell)^2 + 15z^2 - 50z + 24] |a_{\ell}^{(z)}| \quad (16) \end{aligned}$$

Applying this procedure to the linear chain ($z = 2$) without both types of randomness, namely, $h_1 = 0, \Delta = 0$, (9) implies

$$M = Q_{12}(\langle S_1 \rangle + \langle S_2 \rangle) = 2Q_{12}\langle S_1 \rangle = 2Q_{12}M \quad (17)$$

where $Q_{12} = \frac{1}{2} \tanh(2\beta J)$ from relations (13), (14), (15), (16), so that for the respective critical point we get $2Q_{12}^c = 1$ or $\tanh(2\beta_c J) = 1$ which implies that

$$(2\beta_c J)^{-1} = \frac{k_B T_c}{2J} = 0 \quad (18)$$

in accordance with the known exact result for the one-dimensional IM, thus improving on the MFA result that is $(k_B T_c)/J = 2$.

For the disordered square lattice ($z = 4$), the respective Q_{nz} functions are

$$\begin{aligned} Q_{14} &= \frac{1}{2^8}(2G_1 + G_2) \\ Q_{34} &= \frac{1}{2^8}(-2G_1 + G_2) \end{aligned} \quad (19)$$

where $G_k = 3g_{k0} + 4g_{k1} + g_{k2}$ and the g 's functions are defined in (14). The resulting equation for the equilibrium magnetization from (9) is

$$m = 4Q_{14}m + 4Q_{34}m^3 \quad (20)$$

which admits two solutions, the paramagnetic one, $m = 0$, and the ferromagnetic one given by

$$m = \pm \sqrt{\frac{1 - 4Q_{14}}{4Q_{34}}} \quad (21)$$

whereas the critical boundary characterizing the ferromagnetic/paramagnetic phases is determined by the condition $m = 0$ and results as a solution to the equation $4Q_{14} = 1$, which, in case both the random field strength h_1 and exchange integral deviation Δ vanish, then it converts into

$$2 \tanh(2\beta_c J) + \tanh(4\beta_c J) = 2 \quad (22)$$

as was also found in [7], and the critical temperature results as $k_B t_c/J \cong 3.0898\dots$, which is closer to the exact one $k_B t_c^{exact}/J = 2/\ln(1 + \sqrt{2})$ than the MFA one $k_B t_c^{MFA}/J = 4$. At this point, it has to be noted that the decoupling scheme recalled in Eq. (20) behaves as a better approximation than the one in the MFA, since within the EFT framework the kinematics relations are treated exactly ($\sigma^2 = 1$) through the van der Waerden identity; in the present case, EFT neglects correlations only between different spin variables, whereas the MFA neglects any kind of correlation, namely, the self- and multi-spin ones.

3 Numerical results. Phase diagrams. Magnetization profiles

An important feature of the magnetic or fluid systems is their phase diagram, the temperature against a suitably chosen parameter, which, in the present case, allows the investigation more clearly of the effects of randomness itself on the transition temperature of the random system. In the current study,

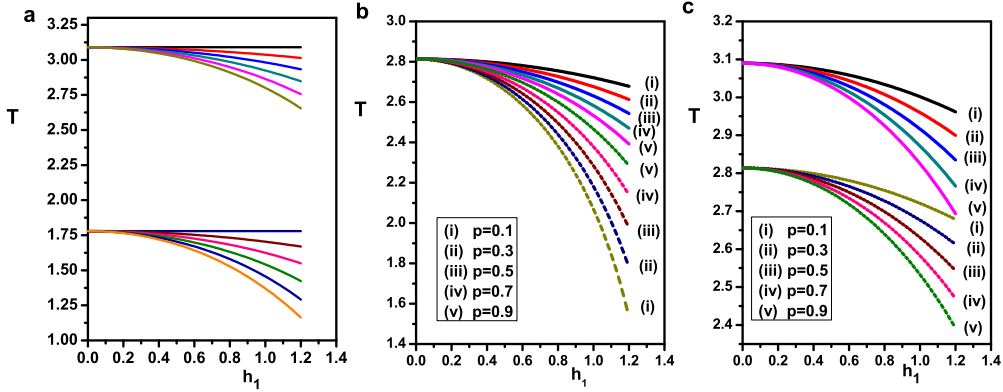


Fig. 1. (Color online) Random field h_1 variation of the critical temperature T - phase diagram ($h_1 - T$). In panel (a), for the upper group of graphs $c = d = 0.0$, for the lower group $c = 0.0$ $d = 1.0$. In each group from up to down $p = 0.0, 0.2, 0.4, 0.6, 0.8, 1.0$. In panel (b), d is fixed as $d = 0.5$, $c = 0.5$ (upper solid graphs), and $c = 1.5$ (lower dashed graphs), labelled by the respective p -values. The solid curves are arranged in increasing p from up to down, whereas the dashed ones are arranged in increasing p from down to up. In panel (c), c is fixed as $c = 0.5$, $d = 0.00001$ upper solid graphs, and $d = 0.5$ lower dashed graphs. The plots in both groups are labelled by the respective p -values. T in units of J/k .

there are various parameters, such as c, Δ, p, h_1 , so that we can introduce a variety of phase diagrams by plotting the temperature with respect to one of these parameters keeping the other ones fixed. However, in the numerical calculations to follow the main quantities β, Δ, h_1, h_2 are written with respect to the average value J of the exchange integral, that is, $\beta \equiv J\beta, d \equiv \Delta/J, h_1 \equiv h_1/J, h_2 \equiv h_2/J$, scaled quantities; this choice influences Eqs. (2) and (3): the PDF in (2) is written as $P(J_{ij}) = \frac{1}{2}\{\delta(J_{ij} - (1 + d)) + \delta(J_{ij} - (1 - d))\}$ so that by choosing $d = 1.0$ the former PDF changes into $P(J_{ij}) = \frac{1}{2}\{\delta(J_{ij} - 2) + \delta(J_{ij})\}$ implying that some of the bonds are missing, diluted bonds. If we also set $c = 0.0$ in Eq. (3), then some of the sites are occupied either by non magnetic particles or are empty, since the respective PDF (3) converts into $P(h_i) = p\delta(h_i - h_1) + q\delta(h_i)$. These cases are shown in Fig 1(a) with each graph labelled by the respective site probability p with the graphs forming two groups: the upper one corresponding to $c = d = 0.0$ (site diluted system with vanishing exchange integral deviation) and the lower group corresponding to $c = 0.0, d = 1.0$, site and bond diluted system. The choice $d = 1.0$ implies that the deviation is of the order of the exchange integral ($d \sim |J|$) so that some bonds may vanish according to the Eq. (2) whereas the remaining ones are strengthened. Also, other phase diagrams are presented in Figs. 1(b,c) with each line labelled by a p -value. In Fig. 1(b), with d fixed as $d = 0.5$, the five upper solid lines correspond to $c = 0.5$, whereas the five lower dashed ones to $c = 1.5$. The topmost solid curve (i) is for $p = 0.1$ and as p increases towards $p = 1.0$, (curve (v)) the respective curve lies below that corresponding to a lower value for p , the higher the p -value the lower the respective curve lies; this

causes a gradual reduction of the ferromagnetic region. As far as the second group is concerned in Fig. 1(b) (dashed ones), an inversion of the order of the curves occurs in comparison to the upper solid ones with respect to p , that is, now the lowermost one (i) corresponds to $p = 0.1$, whereas as p increases towards to $p = 1.0$ (v), the respective line lies above that with a lower value for p , so that, the higher the p -value the higher the curve lies, thus an enlargement of the ferromagnetic region takes place. However, before the inversion of the order of the lines takes place in panel (b), one observes coincidence of the phase-diagram boundaries for the all the p -values for $d = 0.5, c = 1.0$; in this case $h_1 = |h_2|$. However, the order of the curves is unaltered if the temperature T is drawn with respect to the random field h_1 for a fixed value of c ($c = 0.5$), whereas d varies as $d = 0.00001$ (solid curves) and $d = 0.5$ (dashed ones), Fig. 1(c), with the graphs for the same d -value forming a separate group, whereas in Fig. 1(b) they form a single group. A distinctive feature resulting from the plots in Fig. 1 is that all the lines of the phase diagrams coincide for small values of h_1 , beginning from the same point on the T-axis for $h_1 = 0.0$, implying that the critical temperature is the same regardless of c and p but depending only on d . Also, in this figure the critical temperature for $h_1 = 0.0$ is greater the smaller the d -value is. All the critical lines, separating the FM and PM phases, are of second order phase transitions.

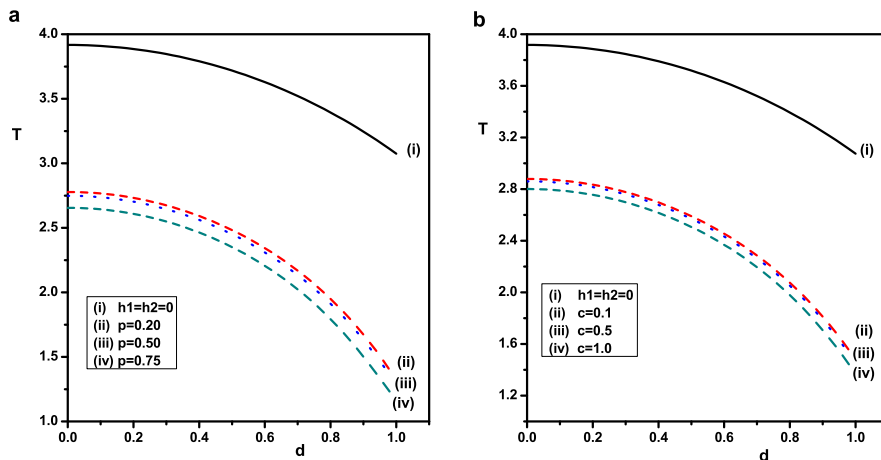


Fig. 2. (Color online) The critical temperature T as a function of the exchange-integral deviation d . In both panels, the upper solid graph (i) corresponds to $h_1 = 0.0$ irrespectively of p (panel (a)) or c (panel (b)). In panel (a), the lower graphs are for fixed c and h_1 as $c = 0.1, h_1 = 1.0$ and labelled by the selected p -values. In panel (b), the lower graphs are for fixed p and h_1 as $p = 0.75, h_1 = 1.0$ and labelled by the selected c -values. In both panels the higher the labeling value the smaller the extent of the ferromagnetic phase.

The dependence of the critical temperature T_c on the exchange-integral deviation $d = \Delta/J$ appears in Fig. 2 for fixed random field $h_1 = 1.0$ as well as for the case $h_1 = 0.0$ for comparison. An overall feature of both panels is that

Table 1

The critical field $h_{1,c}^{(1)}$ – values for constant values $c = 0.5, d = 0$ (second column) and $h_{1,c}^{(2)}$ – values for $c = d = 0.5$ (third column) with respect the parameter p . $h_{1,c}^{(3)}$ refers to the parameter d as a variable with constant values $c = 0.5, p = 0.1$ (fifth column), whereas $h_{1,c}^{(4)}$ refers to the parameter c as a variable with constant values $d = 0.5, p = 0.1$ (seventh column).

p	$h_{1,c}^{(1)}$	$h_{1,c}^{(2)}$	d	$h_{1,c}^{(3)}$	c	$h_{1,c}^{(4)}$
0.0	6.736241	6.194181	0.0	5.904740	0.0	11.124309
0.1	5.900871	5.406162	0.1	5.888921	0.1	9.678039
0.2	4.421102	4.867123	0.2	5.840427	0.2	8.624253
0.3	4.849948	4.435107	0.3	5.758102	0.3	7.543436
0.4	4.488253	4.099344	0.4	5.640081	0.4	6.365760
0.5	4.190953	3.816993	0.5	5.482039	0.5	5.482039
0.6	3.940628	3.572388	0.6	5.277713	0.6	4.768053
0.7	3.725971	3.363212	0.7	5.017263	0.7	4.189970
0.8	3.538211	3.190681	0.8	4.686686	0.8	3.716970
0.9	3.372639	3.053922	0.9	4.269706	0.9	3.324434
1.0	3.224684	2.894779	1.0	3.768020	1.0	2.993567

each line starts from a different point on the T –axis for $d = 0.0$ as compared to Figs. 1. In Fig. 2(a), c was fixed as $c = 0.1$ with the respective curves labelled by a p –value, whereas in Fig. 2(b), the constant quantity was p as $p = 0.75$ with the individual curves labelled by a c –value. In both panels the boundary line for $h_1 = 0.0$ lies above the ones for non zero values of h_1 , thus defining the widest ferromagnetic phase space in comparison to that for non zero h_1 's implying that the effect of including the random field is to reduce the ferromagnetic region; also the boundaries are arranged one below the other in ascending order either for p or c so that each time p or c is increased the respective ferromagnetic region is reduced in comparison to that with a smaller p or c .

The critical field $h_{1,c}$, the field for which the critical temperature vanishes, depends on the thermodynamic route followed, since the current random system contains various parameters, namely, c, d, p ; consequently, in order to estimate $h_{1,c}$, two of these parameters are fixed, only the remaining one varies. Initially, c and d are kept fixed as $c = 0.5, d = 0$ and later $c = d = 0.5$; the values of the respective critical field $h_{1,c}$ appear in Table 1 for selected p –values for both choices. In the former case, these values are fitted by the sixth-degree polynomial $P(x) = 6.73612 - 9.97119x + 19.00728x^2 - 30.76579x^3 + 33.56416x^4 - 20.72121x^5 + 5.37542x^6$, whereas in the latter case by the fifth-degree poly-

mial $P(x) = 6.19323 - 9.39129x + 18.25539x^2 - 27.81661x^3 + 23.72744x^4 - 8.07256x^5$, with $x \equiv p$ in both cases. Also, in the same Table, there appear the values for the critical field $h_{1,c}^{(3)}$ (fifth column) corresponding to the constant quantities $c = 0.5, p = 0.1$ with parameter d as a variable, for which the best fit polynomial is $P(x) = 5.90487 - 1.6687x^2 + 0.39594x^3 - 0.8657x^4$ ($x \equiv d$); moreover, in the seventh column there appear the values for the critical field $h_{1,c}^{(4)}$ corresponding to the constants $d = 0.5, p = 0.1$ and parameter c as a variable, with best fit polynomial $P(x) = 11.12544 - 14.35749x + 6.410899x^2 - 0.155474x^4$ ($x \equiv c$).

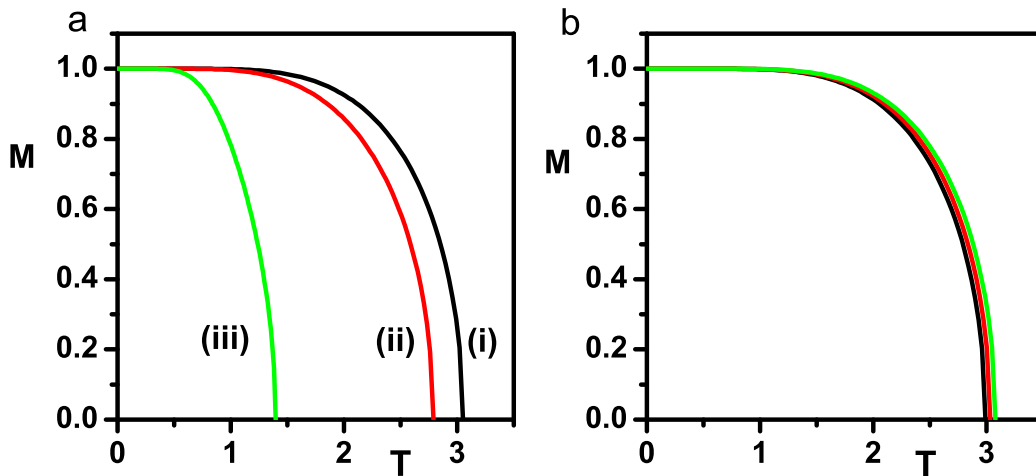


Fig. 3. (Color online) The thermal dependence of magnetization $M(T, h_1)$, order parameter. In panel (a), the fixed parameters are $d = 0.1, p = 0.1, h_1 = 1.0$; each graph is labelled by the random field ratio $c = h_2/h_1$: $c = 0.1$ graph (i), $c = 1.0$ graph (ii) and $c = 2.0$ graph (iii). In panel (b), the fixed parameters are $c = 3.0, d = 0.1$; each graph is labelled by p and h_1 as: innermost graph $p = 0.1, h_1 = 0.2$, middle one $p = 0.6, h_1 = 0.2$ and outermost $p = 0.1, h_1 = 0.0$.

In addition to the phase diagram, another important quantity is the magnetization; its thermal behavior appears in Fig. 3 for various values of the system's parameters c, d, p, h_1 , resulting by solving numerically the Eq. (20). In panel (a) the parameters d, p, h_1 are fixed as $d = 0.1, p = 0.1, h_1 = 1.0$; the individual graphs are labelled by the random field ratio $c = h_2/h_1$, the outermost graph (i) corresponds to $c = 0.1$, the middle one (ii) to $c = 1.0$ and the innermost one (iii) to $c = 2.0$. The magnetization exhibits its normal behavior but it is stronger for the smaller value of this parameter $c = 0.1$ (for $c = 0.0$ the respective graph is very close to that for $c = 0.1$ due to the finiteness of the calculations), which is in accordance with the respective plot in Ref. [12] although in the latter publication the random field is not included. In the latter case ($c = 2.0$) the stronger negative random field $h_2 = ch_1$ yields smaller magnetization because this field competes strongly the first term in the Hamiltonian (1), which favors the parallel orientation of the spins. In panel (b) the parameters c, d, h_1 are fixed as $c = 3.0, d = 0.1, h_1 = 0.2$,

the plots are labelled by the site probability $p = 0.1$ (innermost graph) and $p = 0.6$ for the middle graph; for comparison the case for the lack of the random field was also included, which is the outermost graph corresponding to $c = 3.0, d = 0.1, p = 0.1, h_1 = 0.0$. For small values of the temperature, the magnetization values are constant, independent of the relative parameters.

A susceptibility-like quantity $\chi_T(h_1)$ can also be calculated as the first order derivative of the magnetization with respect to the applied external random magnetic field, namely

$$\chi_T(h_1) = \frac{\partial m}{\partial h_1} = \frac{\partial m}{\partial h_0} \frac{dh_0}{dh_1} = \frac{1}{J} \frac{\partial m}{\partial h_0} \quad (23)$$

so that

$$J\chi_T(h_1) = \frac{\partial m}{\partial h_0} = \frac{4m \frac{\partial Q_{14}}{\partial h_0} + 4m^3 \frac{\partial Q_{34}}{\partial h_0}}{1 - 4Q_{14} - 12m^2 Q_{34}} \quad (24)$$

or, for calculational purposes,

$$\left(J\chi_T(h_1)\right)^{-1} = \frac{1 - 4Q_{14} - 12m^2 Q_{34}}{4m \frac{\partial Q_{14}}{\partial h_0} + 4m^3 \frac{\partial Q_{34}}{\partial h_0}} \quad (25)$$

since $h_0 = Jh_1$, although the product (Jh_1) was earlier set as h_1 , now we divert for calculational purposes.

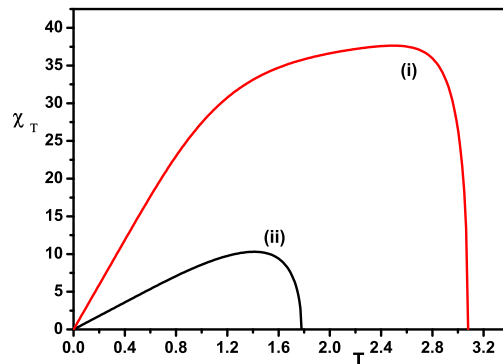


Fig. 4. (Color online) The inverse magnetic susceptibility-like vs temperature T , with constant $c = p = h_1 = 0.1$; graph (i) corresponds to $d = 0.1$ and graph (ii) to $d = 1.0$.

The temperature dependence of the inverse susceptibility-like is shown in Fig. 4 for selected values of the parameters c, d, p, h_1 . In both graphs, the susceptibility diverges twice, once at the zero temperature ($T = 0$, finite clusters

contribution) and once again at the respective critical point T_c , infinite cluster contribution. Although both graphs increase smoothly for small T -values, they decrease steeply for larger ones. A similar behavior for the susceptibility was also found by Kaneyoshi et al [24].

4 Conclusions and discussions

In the current investigation we have determined the phase diagrams, critical temperatures, magnetization profiles and susceptibility of the nearest-neighbor spin-1/2 Ising model on a square lattice, in the presence of competing random fields as well as fluctuating random bonds via EFT, based on the differential operator technique and Callen identity. The topology of the system is taken into account through the coordination number. The EFT method is an improvement on the MFA, since it provides vanishing critical temperature for one-dimensional systems, also for two-dimensional systems the respective critical temperature is closer to the exact one than that of the MFA. A variety of phase diagrams were obtained with respect to the various system's parameters, namely, c, d, h_1, p . The extent of the ferromagnetic region does not show systematic variation on varying the system's parameters; it varies non monotonically for constant d and varying c , whereas in other circumstances it varies monotonically. The magnetization profile was determined with respect to temperature as well as the random field h_1 . An immediate result of the presence of the random field is to reduce the extent of the ferromagnetic region, in general, as well as numerical value of the magnetization as c increases because of the strengthening of the random field $h_2 = ch_1$ and the subsequent increased tendency of this field to prevent spins to attain the parallel configuration and the competition with the other random field h_1 .

Although the EFT technique improves on the MFA, it presents the same shortcomings in the critical region (non-classical region) concerning the critical exponents like the MFA and Landau theory, because the fluctuations occurring in the critical region, as the transition temperature is approached, become important and the non-classical behavior is observed; these fluctuations are not taken under consideration properly by EFT or MFA, thus a relative criterion, called Ginzburg criterion, determines how close to the transition temperature the true critical behavior is revealed [25]. This criterion relies on any thermodynamic quantity but the specific heat is usually considered for determining the critical region around T_c where the mean field solution cannot describe correctly the phase transition. The MFA is valid for lattice dimensionality greater than the upper critical dimension $d_u = 4$ in case of presence of only thermal fluctuations. However, in the current case the presence of random fields enhances fluctuations causing the critical region to be wider than the one due only to the thermal fluctuations and the upper critical dimension is increased by 2 to $d_u = 6$ [26,27]. Occasionally the non classical region is extremely narrow so that the respective critical behavior expected by Landau

or MFA is observed because the fluctuation region is very narrow and hardly accessible for experimental observation; such a system is the weak-coupling superconductor in three dimensions for which the respective non classical region is $|t_{CR}| \leq 10^{-16}$ (t_{CR} is the reduced temperature). However, on reducing the space dimension as in the case of the weak-coupling superconductor in two dimensions, the critical exponents have their classical values up to $|t_{CR}| = 10^{-5}$, thus the reduction of the space dimensionality causes serious repercussions on the behavior of the physical system; on the contrary, for the superfluid helium transition the classical region extends up to $|t_{CR}| \leq 1.0$ so that fluctuations are detectable [28,29,30,31]. In addition to superconductivity, the extent of the non classical region for the ferroelectric system triglycine sulfate (TGS) is relatively small and its critical exponents have the respective classical values up to $|t_{CR}| = 1.5 \times 10^{-5}$ [32,33,34].

The results obtained in the current investigation by using the EFT provide a basis for a comprehensive analysis by more sophisticated methods. However, they are of no less importance, since they show, nevertheless, the expected phenomena to be observed.

Acknowledgements

This research was supported by the Special Account for Research Grants of the University of Athens (*EAKKE*) under Grant No. 70/4/4096.

References

- [1] I. A. Hadjiagapiou, A. Malakis, S. S. Martinos, *Physica A* 387 (2008) 2256.
- [2] I. A. Hadjiagapiou, *Physica A* 390 (2011) 1279.
- [3] K. Hui, A. Nihat Berker, *Phys. Rev. Lett.* 62 (1989) 2507.
- [4] I. A. Hadjiagapiou, *Physica A* 390 (2011) 3204.
- [5] R. Honmura, T. Kaneyoshi, *J. Phys. C* 12 (1979) 3979.
- [6] H. B. Callen, *Phys. Lett.* 4 (1963) 161.
- [7] E. F. Sarmiento, C. Tsallis, *Phys. Rev. B* 27 (1983) 5784.
- [8] E. F. Sarmiento, C. Tsallis, R. Honmura, *Phys. Rev. B* 31 (1985) 3153.
- [9] T. Kaneyoshi, I. P. Fittipaldi, H. Beyer, *Phys. Status Solidi B* 102 (1980) 393.
- [10] T. Kaneyoshi, I. Tamura, R. Honmura, *Phys. Rev. B* 29 (1984) 2769.
- [11] G. B. Taggart, *Physica A* 116 (1982) 34.
- [12] T. Kaneyoshi, I. Tamura, *Phys. Rev. B* 25 (1982) 4679.
- [13] S. M. Zheng, *Phys. Rev. B* 52 (1995) 7260.
- [14] Y. Yüksel, Ü. Akinci, H. Polat, *Physica A* 391 (2012) 415.
- [15] T. Kaneyoshi, *Phys. Status Solidi B* 248 (2011) 250.
- [16] A. Aharony, *Phys. Rev. B* 18 (1978) 3318.
- [17] D. Andelman, *Phys. Rev. B* 27 (1983) 3079.
- [18] M. Kaufman, M. Kanner, *Phys. Rev. B* 42 (1990) 2378.
- [19] S. Fishman, A. Aharony, *J. Phys. C: Solid St. Phys.* 12 (1979) L729.
- [20] J. Z. Imbrie, *Phys. Rev. Lett.* 53 (1984) 1747.
- [21] M. Gofman, J. Adler, A. Aharony, A. B. Harris, M. Schwartz, *Phys. Rev. Lett.* 71 (1993) 2841; *Phys. Rev. B* 53 (1996) 6362.
- [22] A. Houghton, A. Khurana, F. J. Seco, *Phys. Rev. B* 34 (1986) 1700.
- [23] J. Machta, M. E. J. Newman, L. B. Chayes, *Phys. Rev. E* 62 (2000) 8782.
- [24] T. Kaneyoshi, R. Honmura, I. Tamura, E. F. Sarmiento, *Phys. Rev. B* 29 (1984) 5121.
- [25] V. L. Ginzburg, *Fiz. Tverd. Tela. (Leningrad)* 2 (1960) 2031 [*Sov. Phys.-Solid State* 2 (1961) 1824].
- [26] M. Kaufman, M. Kardar, *Phys. Rev. B* 31 (1985) 2913.

- [27] J. Als-Nielsen, R. J. Birgeneau, *Amer. J. Phys.* 45 (1977) 554.
- [28] A. Z. Patashinskii, V. I. Pokrovskii, *Fluctuation Theory of Phase Transitions*, Pergamon Press, Oxford, U.K., 1979.
- [29] Y. M. Ivanchenko, A. A. Lisyansky, *Physics of Critical Fluctuations*, Springer-Verlag, New York, U.S.A, 1995.
- [30] C. Domb, *The Critical Point: A Historical Introduction to the Modern Theory of Critical Phenomena*, Taylor and Francis, London, U.K., 1996.
- [31] N. Goldenfeld, *Lectures On Phase Transitions And The Renormalization Group*, Addison-Wesley, Reading, Ma, 1992.
- [32] K. Deguchi, E. Nakamura, *Phys. Rev. B* 5 (1972) 1072.
- [33] A. Mercado, J. A. Gonzalo, *Phys. Rev. B* 7 (1973) 3074.
- [34] T. Mitsui, E. Nakamura, M. Tokunaga, *Ferroelectrics* 5 (1973) 185; M. Tokunaga, T. Mitsui, *Ferroelectrics* 11 (1976) 451.